Postmillennium changes in stratospheric temperature consistently resolved by GPS radio occultation and AMSU observations

Sergey Khaykin, Beatriz M. Funatsu, Alain Hauchecorne, Sophie Godin-Beekmann, Chantal Claud, Philippe Keckhut, Andrea Pazmino, Hans Gleisner, Johannes K. Nielsen, Stig Syndergaard, et al.

AGU PUBLICATIONS

Geophysical Research Letters

RESEARCH LETTER
10.1002/2017GL074353

Key Points:
- Stratospheric temperature trends derived from GPS-RO and Aqua AMSU observations 2002–2016 are in excellent agreement
- Middle stratosphere has cooled in the time period 2002–2016 at an average rate of −0.14 to −0.36 K/decade
- The spatially and seasonally resolved trends indicate changes in the stratospheric circulation

Supporting Information:
- Supporting Information S1

Correspondence to:
S. M. Khaykin,
sergey.khaykin@latmos.ipsl.fr

Citation:
Khaykin, S. M., et al. (2017), Postmillennium changes in stratospheric temperature consistently resolved by GPS radio occultation and AMSU observations, *Geophys. Res. Lett.*, *44*, 7510–7518, doi:10.1002/2017GL074353.

Received 31 MAY 2017
Accepted 14 JUL 2017
Accepted article online 20 JUL 2017
Published online 27 JUL 2017

Postmillennium changes in stratospheric temperature consistently resolved by GPS radio occultation and AMSU observations

S. M. Khaykin[1], B. M. Funatsu[2], A. Hauchecorne[1], S. Godin-Beekmann[1], C. Claud[1,3], P. Keckhut[1], A. Pazmino[1], H. Gleisner[4], J. K. Nielsen[4], S. Syndergaard[4], and K. B. Lauritsen[4]

[1]LATMOS/IPSL, UVSQ Université Paris-Saclay, UPMC University Paris 06, CNRS, Guyancourt, France, [2]CNRS, Université de Nantes, LETG UMR 6554, Nantes, France, [3]LMD/IPSL, CNRS UMR 8539, École Polytechnique, Université Paris Saclay, ENS, PSL Research University, Sorbonne Universités, UPMC Univ Paris 06,CNRS, Palaiseau, France, [4]Danish Meteorological Institute, Copenhagen, Denmark

Abstract Temperature changes in the lower and middle stratosphere during 2001–2016 are evaluated using measurements from GPS Radio Occultation (RO) and Advanced Microwave Sounding Unit (AMSU) aboard the Aqua satellite. After downsampling of GPS-RO profiles according to the AMSU weighting functions, the spatially and seasonally resolved trends from the two data sets are in excellent agreement. The observations indicate that the middle stratosphere has cooled in the time period 2002–2016 at an average rate of −0.14 ± 0.12 to −0.36 ± 0.14 K/decade, while no significant change was found in the lower stratosphere. The meridionally and vertically resolved trends from high-resolution GPS-RO data exhibit a marked interhemispheric asymmetry and highlight a distinct boundary between tropospheric and stratospheric temperature change regimes matching the tropical thermal tropopause. The seasonal pattern of trend reveals significant opposite-sign structures at high and low latitudes, providing indication of seasonally varying change in stratospheric circulation.

Plain Language Summary Stratosphere is an important part of the Earth climate system. Long-term change in stratospheric temperature is a key indicator of global climate change, reflecting both natural and anthropogenic forcings. A variety of long-term observations and models indicate a cooling throughout the stratosphere in response to ozone depletion and growing emissions of greenhouse gases. This study exploits two independent sets of satellite observations by Advanced Microwave Sounding Unit (AMSU) and GPS radio occultation (RO). We find excellent agreement between spatially and seasonally resolved trends from the two data sets, which provides confidence in our estimates. The observations indicate a statistically significant global cooling in the middle stratosphere since 2001 at a mean rate of −0.14 to −0.36 K/decade and insignificant change in the lower stratosphere. The seasonal and spatial patterns of trend provide indication of seasonally varying change in stratospheric circulation. We argue that GPS-RO technique, featuring certain advantages over other atmospheric observing systems, provides a more detailed view of the stratospheric temperature change thereby allowing a better understanding of the underlying forcing mechanisms. Future RO missions will continue the existing record, potentially becoming the primary source of information on the lower stratospheric temperature in the 21st century.

1. Introduction

Stratospheric temperature trends represent a key indicator of global climate change, reflecting both natural and anthropogenic forcings. A variety of long-term observations and models indicate a cooling throughout the stratosphere in response to ozone depletion and growing emissions of greenhouse gases (see reviews by *Randel et al.* [2009] and *Seidel et al.* [2011]). While ground-based observations provide the longest records of stratospheric temperatures, space-borne data records—spanning nearly four decades—provide global coverage. The spatial and seasonal patterns of trend inferred from satellite observations are essential for monitoring changes that arise from the combination of different forcings [*Ramaswamy et al.*, 2001].

The longest satellite-based climate data records (CDR) on stratospheric temperatures are provided by operational nadir sounders measuring long-wave emission from broad atmospheric layers, defined by the appropriate instrument weighting functions. Stratospheric Sounding Unit (SSU) and Microwave Sounding Unit (MSU) flown aboard a series of NOAA polar-orbiting satellites during 1979–2005, followed by Advanced

Microwave Sounding Unit (AMSU) operational since 1998, provided multidecadal observations that have lent themselves to a number of stratospheric temperature change surveys reviewed by *Seidel et al.* [2011]. However, because these instruments were conceived primarily for operational weather forecasting [*Randel et al.*, 2009], their application for long-term climate monitoring has resulted in conflicting trend estimates [*Thompson et al.*, 2012]. A substantial effort has been undertaken to reconcile these differences by accounting for time-varying biases and homogenization of data sets from different nadir sensors [*Zou et al.*, 2014; *Wang and Zou*, 2014; *Zou and Qian*, 2016]. The cease of SSU operation in 2006 increased the need for merging CDRs from different sensors and fostered combined use of nadir and limb-sounding observations [*McLandress et al.*, 2015; *Randel et al.*, 2016]. In addition, limb-sounding instruments provide a far more detailed information on the vertical structure of the trends, inaccessible to nadir sounders sampling broad atmospheric layers.

The call for new stratospheric temperature CDRs is addressed by the GPS Radio Occultation (RO) technique, providing an independent upper air record of potentially benchmark quality [*Leroy et al.*, 2006]. GPS-RO exploits the signals emitted by GPS satellites in a limb-sounding geometry. An intrinsic long-term stability of measurements render RO observations particularly valuable for climate monitoring, as demonstrated in various studies [*Steiner et al.*, 2007; *Foelsche et al.*, 2008; *Scherllin-Pirscher et al.*, 2011]. Continuous RO measurements are available since 2001, and several studies have already used these data to quantify the changes in stratospheric temperature [*Steiner et al.*, 2009; *Ladstädter et al.*, 2011].

Our study advances the previous work using the most recent GPS-RO data set spanning slightly more than 15 years. The consistency of RO-based trends and their seasonal and spatial structures are verified through comparison with Aqua AMSU observations covering roughly the same period. The overall aim is to accurately quantify the pattern of lower and middle stratospheric temperature change in the early 21st century using two independent CDRs.

2. Data and Methods

2.1. AMSU

AMSU is a nadir cross-scanning microwave sounder operating on board the NOAA, Aqua, and Metop satellites since late 1998. AMSU channels 9–14 sample at or above the tropopause, with weighting functions peaking at approximately 18, 21, 26, 31, 37, and 42 km, respectively (Figure S1 in the supporting information). Each weighting function has a half-power vertical range of ~10 km. While Aqua and Metop platforms are kept at nearly constant orbits, NOAA satellites drift with time, which has important implications for trend estimation linked to solar tide effects [*Keckhut et al.*, 2015]. For this reason, we opt to use AMSU data from Aqua, which has the longest time series among the nondrifting satellites providing data since mid-2002.

We use the NOAA STAR Integrated Microwave Inter-Calibration Approach (IMICA) version of the data as it is better suited for climate applications [*Zou and Wang*, 2011; *Zou et al.*, 2013]. Our analysis exploits the brightness temperature measurements from the inner 10 fields of view, covering a swath of ~500 km. More details on Aqua AMSU can be found in *Funatsu et al.* [2016, and references therein].

2.2. GPS Radio Occultation

The GPS-RO technique provides profiles of atmospheric variables in the troposphere and lower/middle stratosphere with high vertical resolution (~0.5 to 1.5 km), global geographical and full diurnal coverage, and high accuracy ($<$1 K) [*Steiner et al.*, 1999; *Kursinski et al.*, 1997]. As demonstrated in various studies [*Ho et al.*, 2009; *Foelsche et al.*, 2009, 2011], RO data from different sensors and missions can be combined without intercalibration as long as the same data processing chain is used. We use RO data from the EUMETSAT RO Meteorology Satellite Application Facility (ROM SAF). The analysis is based on a recent ROM SAF reprocessing, which incorporates measurements from four RO missions: CHAMP [*Wickert et al.*, 2004]; FORMOSAT-3/COSMIC [*Anthes et al.*, 2008]; GRACE [*Beyerle et al.*, 2005], and Metop [*Luntama et al.*, 2008]. The available data covers the period from September 2001 to December 2016 and incorporates nearly 9 million quality-checked profiles. The time span and monthly number of occultations for each mission is provided in Figure S2.

We use "dry" temperature profiles (temperatures retrieved under the assumption of negligible humidity) within altitude range 10–35 km interpolated onto a common 0.5 km vertical grid. For constructing temperature climatologies from GPS-RO data, one commonly accounts for sampling errors resulting from uneven geographical sampling. This is particularly important for the single-satellite CHAMP mission, characterized by relatively

sparse spatial sampling. Following *Foelsche et al.* [2008], we estimate the sampling errors using ERA-Interim reanalyses, by subtracting a constructed climatology based on the full set of ERA-Interim data, from a climatology constructed using only ERA-Interim profiles interpolated to RO observation locations.

2.3. Setup of Data and Linear Trend Computation

The temperature anomalies for each data set are derived by averaging measurements into 5° latitude bins before weighting the binned data by the cosine of latitude to account for the variable area of latitude bands. The linear trends are then computed using robust regression on deseasonalized zonal-mean monthly averages (anomalies). The robust method [*Rousseeuw and Leroy*, 2005] reduces the sensitivity of trend estimation to strong temperature departures caused by extreme dynamical events such as sudden stratospheric warmings. Statistical uncertainties are quoted with either $\pm 2\sigma$ (≈95% confidence) or $\pm 1\sigma$ (≈67% confidence).

In order to match the vertical resolution of GPS-RO with that of AMSU, the profiles of the former are vertically averaged using weighting functions of AMSU channels 9–12 following the procedure described by *McLandress et al.* [2015]. The vertical averaging was performed with the limits of integration corresponding to the RO vertical range, i.e., 10–35 km. For intercomparison, the time period of the GPS-RO data was restricted to the span of the available Aqua AMSU record—August 2002 through August 2016, and its zonal coverage, 85°S to 85°N.

3. Intercomparison of Trends From AMSU and GPS-RO

Figure 1 shows the latitude variation of the trends derived from both CDRs after reduction of GPS-RO profiles to AMSU vertical resolution. The vertically resolved trends from GPS-RO and AMSU are in remarkable agreement with the differences below 0.15 K/decade for all layers (channels) and latitude bands. The errors of AMSU and GPS-RO trends are in fair agreement, with the latter being somewhat lower in the tropical bands and both data sets reflecting higher dynamical variability in the polar regions. Both AMSU and GPS-RO show considerable variation of trends as a function of layer at all latitude bands except Northern Hemisphere (NH) high latitudes. The vertical structure of the trends at middle and low latitudes exhibits stronger cooling toward the upper layers. The largest and statistically significant (2σ level) cooling trends are observed in the upper channels (11 and 12) at SH midlatitudes and the tropical bands. The lower channels (9 and 10) show insignificant cooling throughout the extratropics and small but significant warming in the tropical bands, where AMSU-9 weighting function extends well into the tropical upper troposphere.

The global trends, provided in the embedded panel in Figure 1, confirm the consistency between AMSU and GPS-RO series, revealing nearly identical trend values with the largest difference (0.04 K/decade) corresponding to channel 9. The vertical structure of the global trends is such that channel 9 shows virtually no temperature change, whereas channels 10 to 12 show little yet significant (2σ) cooling increasing in absolute value with altitude from -0.14 ± 0.12 to -0.36 ± 0.14 K/decade. The good agreement between AMSU and GPS-RO trends for channel 12 despite the incomplete coverage of this layer by GPS-RO (Figure S1) could be due partly to the close proximity of trend values for AMSU-12 (-0.37 K/decade) and the overlying AMSU-13 (-0.39 K/decade, not shown in Figure 1). This way, the invariant temperature trend for AMSU-12 and AMSU-13 minimizes the effect of incomplete vertical coverage by GPS-RO on the trend estimate for channel 12.

A better insight into the data underlying the trends is provided in Figure 2, comparing the global temperature anomalies for channel 10. The AMSU weighting function for channel 10 is entirely within the chosen vertical range of GPS-RO data (10–35 km, Figure S1) and is therefore most suitable for comparison. The temperature anomalies from AMSU and GPS-RO are in excellent agreement throughout the comparison period. Similar results are obtained for the other channels (not shown). We also note that the GPS-RO and AMSU negative trends, which corroborate each other, appear to be more pronounced at the beginning of the 15 year period.

The mean difference between the anomalies (GPS-RO minus AMSU) is 0.06 ± 0.10 K (1 standard deviation) for channel 10 and does not exceed $|0.08| \pm 0.12$ K for any other channel. We found that the much sparser GPS-RO sampling during the CHAMP era (i.e., before June 2006) does not lead to larger differences between GPS-RO and AMSU climatologies, as the mean anomaly difference for the periods of low and high sampling is virtually the same (0.064 ± 0.12 K and 0.065 ± 0.09 K, respectively). It is noteworthy that without application of the sampling error correction to GPS-RO data, the mean anomaly difference over the CHAMP period is notably higher and amounts to 0.1 ± 0.16 K.

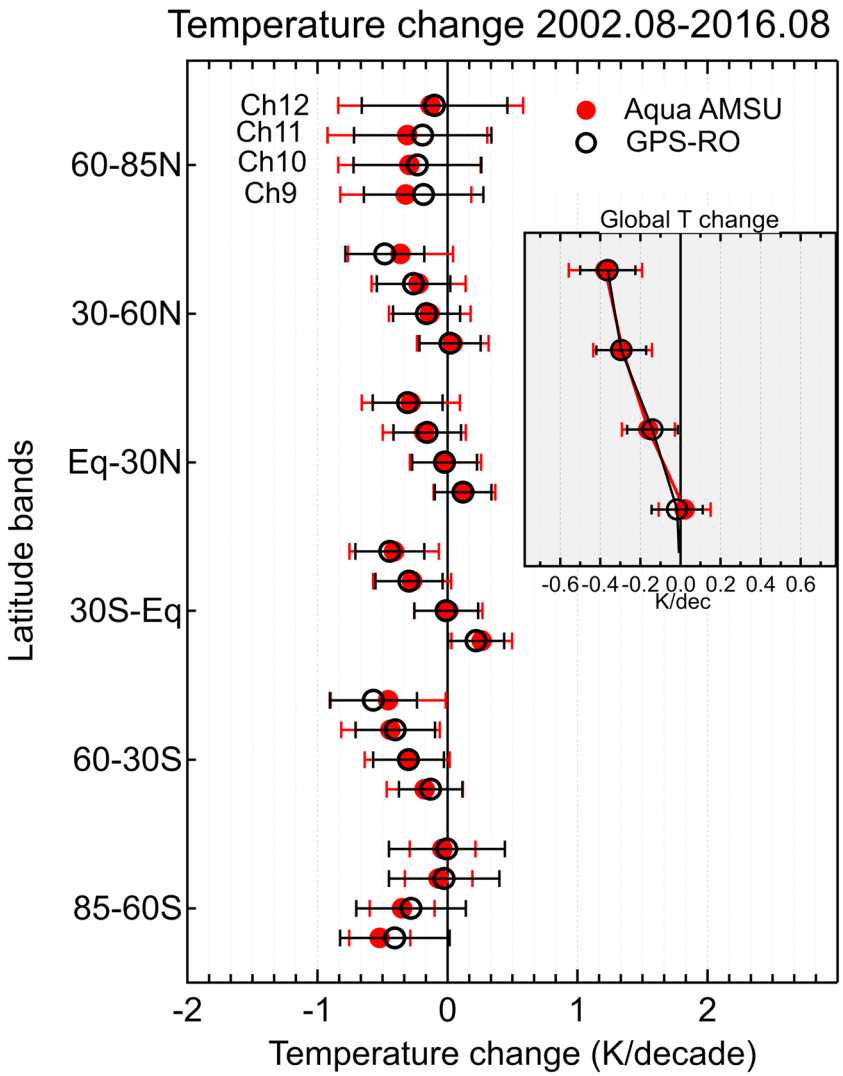

Figure 1. Vertical structure of temperature trends derived from AMSU and GPS-RO data for the period August 2002 to August 2016. The vertical layers correspond to AMSU channels 9 to 12. The main panel displays the trends by latitude bands (shown in the ordinates), the embedded panel displays global trends. Error bars represent 2σ uncertainty estimates.

Having established the consistency between AMSU and GPS-RO temperature trends as a function of latitude and vertical layer, we examine their seasonal structures. For that, we again focus on the data corresponding to AMSU channel 10, which samples the lower stratosphere (LS) while being less affected by the tropical upper troposphere than channel 9.

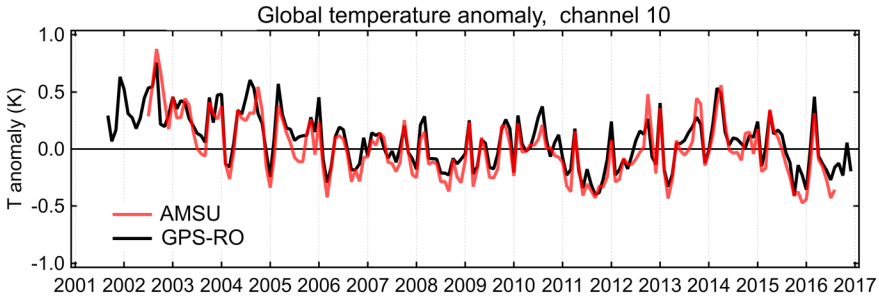

Figure 2. Global temperature anomalies from AMSU and GPS-RO in the vertical layer corresponding to the AMSU-10 weighting function peaking at ~21 km.

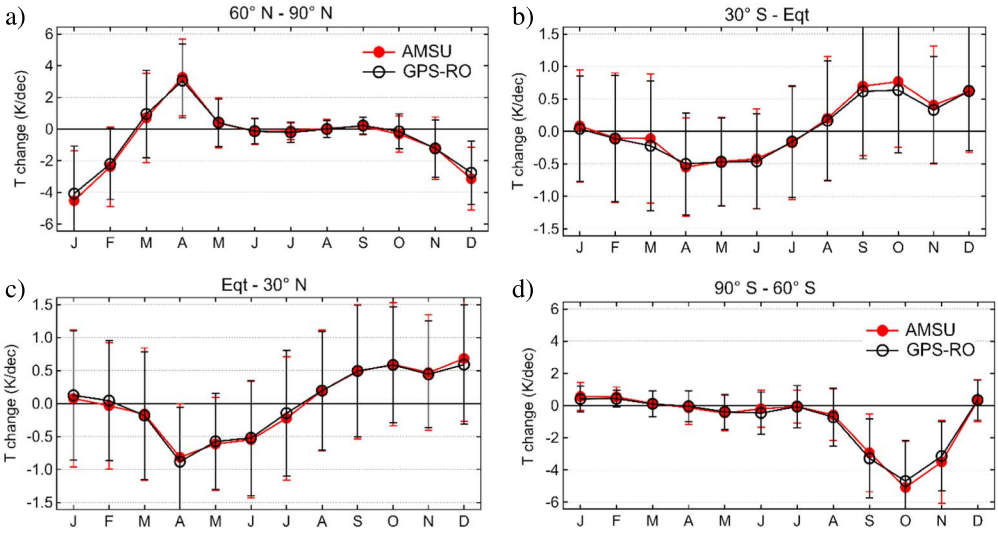

Figure 3. Trends by month from AMSU and GPS-RO data for the vertical layer corresponding to channel 10 for the latitude bands (a) 60°N–90°N; (b) 0°–30°N; (c) 30°S–0°; and (d) 90°S–60°S. Error bars represent 2σ uncertainty estimates.

Figure 3 shows channel 10 trends from AMSU and GPS-RO estimated independently for each calendar month for low- and high-latitude bands in both hemispheres. The seasonal patterns from the two data records are in excellent agreement. The corresponding uncertainties, reflecting the variance of temperature anomalies in a given calendar month, are largely consistent as well. Although all tropical monthly trends and a majority of polar trends are insignificant at the 2σ level, there is a pronounced seasonality of temperature change.

The tropical trends in the NH (Figure 3b) and SH (Figure 3c) exhibit a similar seasonality with (1σ) significant cooling in April–June and warming in September–December. The seasonal pattern of polar trends is more pronounced and features (2σ) significant cooling of −3 to −5 K/decade during northern winter (Figure 3a) and southern spring (Figure 3d), which is contrasted by a significant warming in the Arctic restricted to April (Figure 3a). The summer months at polar latitudes show much smaller year-to-year variability (reflected by the error bars) as well as near-zero change. The other channels reveal similar seasonal patterns (not shown).

4. Vertically Resolved Trends From the 15 Year GPS-RO Data Record

The consistency of two independent observational data records, as demonstrated in the previous section, provides a certain confidence in the estimates of global and spatially (seasonally) resolved trends. It is noteworthy that a correct AMSU-GPS-RO intercomparison would not have been possible without

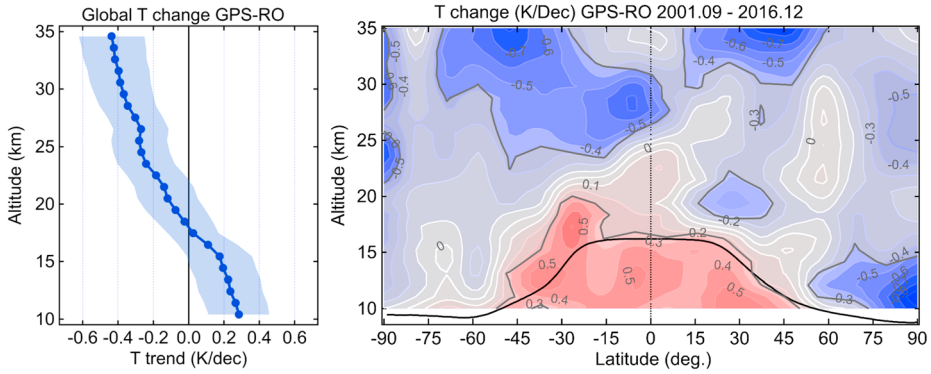

Figure 4. (left) Global-mean trend from GPS-RO for the period September 2001 to December 2016 from GPS-RO. Blue shading represents 2σ uncertainty estimate. (right) Latitude-altitude pattern of temperature trend from GPS-RO at 1 km vertical resolution for the same period. Contour interval is 0.1 K/decade. The gray shading conceals trends that are insignificant at the 2σ level. The solid black line indicates the climatological thermal (lapse rate) tropopause derived from the GPS-RO data.

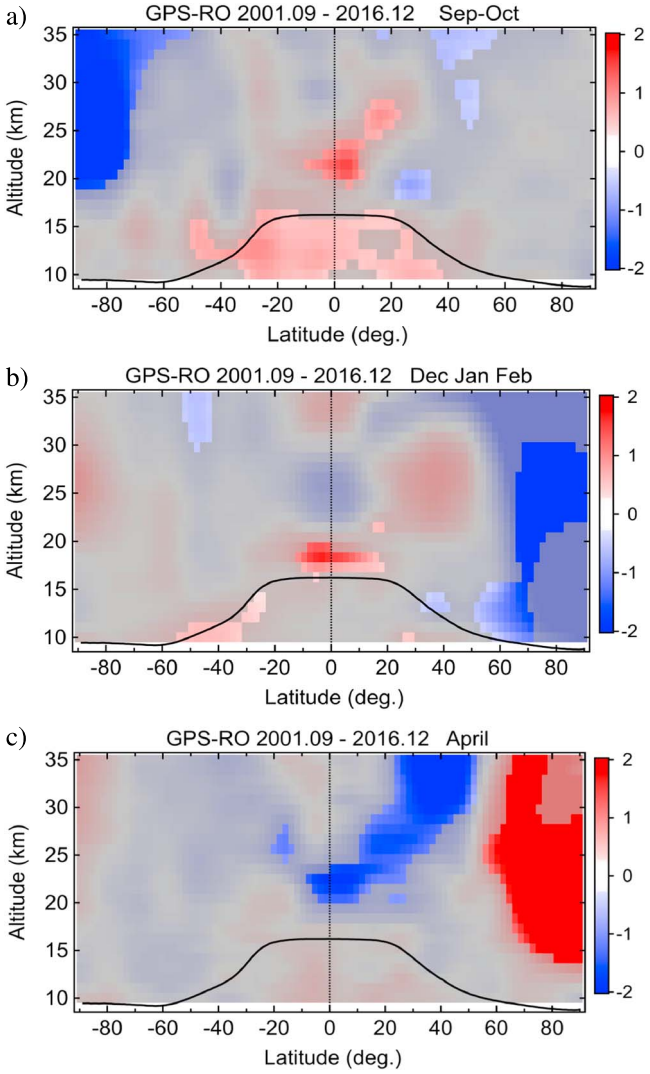

Figure 5. Latitude-altitude pattern of trend (in K/decade) for the period September 2001 to December 2016 from GPS-RO for the selected seasons/month: (a) September–October; (b) December–February; and (c) April. The solid black line indicates the climatological thermal tropopause derived from GPS-RO data.

downsampling GPS-RO vertical profiles to match the broad stratospheric layers sampled by the AMSU nadir sounder. In this section, we take advantage of the high vertical resolution of GPS-RO measurements spanning September 2001 to December 2016 to determine the trend patterns at 1 km vertical resolution inaccessible by the nadir sounders.

Figure 4 (left) shows the vertical structure of global-mean trends from GPS-RO. A significant warming trend reaching 0.29 ± 0.17 K/decade is observed below 14 km. A change from warming to cooling regime is found at ~18 km, and the negative trend increases with altitude obtaining statistical significance at ~22 km and reaching its maximum value of 0.44 ± 0.19 K/decade at 35 km.

A better insight into the stratospheric temperature change is provided by the latitude-altitude section of trends, displayed in Figure 4 (right). The grey shading conceals the areas where the trends are insignificant at the 2σ level. The tropical thermal tropopause (black curve, derived from GPS-RO data) highlights a distinct boundary between tropospheric and stratospheric temperature change regimes, i.e., significant warming in the troposphere [*Thorne et al.*, 2010] and meridionally variable change above the tropopause. In the lower stratosphere, the trend pattern reveals two distinct areas of warming and cooling in the southern and northern subtropics, respectively, as well as an area of strong cooling in the NH polar region, not observed in the SH. These areas of significant temperature change have a vertical extent of a few kilometers only and therefore cannot be correctly resolved by AMSU. In the midstratosphere, SH cooling has a larger meridional and vertical extent compared to that in the NH.

The next step is to examine the contribution of different seasons to the observed latitude-altitude trends. The seasonal dependence of the trend patterns is to be interpreted through consideration of the stratospheric circulation and its relation with the temperature. There exists an out-of-phase relationship between the tropical and extratropical temperature variations, which is commonly associated with the Brewer-Dobson Circulation (BDC) [*Yulaeva et al.*, 1994]. Driven by extratropical wave forcing, BDC draws the air upward from the tropics and downward at middle to high latitudes, rendering the temperatures respectively cooler and warmer than their radiative equilibrium [e.g., *Shine*, 1987]. The acceleration of BDC leads to additional cooling in the lower tropical stratosphere and warming at high latitudes, whereas the opposite is true if the BDC is weakening [e.g., *Thompson and Solomon*, 2005]. Because BDC is strongest in the winter and spring in both hemispheres [e.g., *Holton et al.*, 1995], its interannual change is most prominent during these seasons [*Fu et al.*, 2010; *Young et al.*, 2012].

In the previous section, we showed that the temperature change in the lower stratosphere has a pronounced seasonality with the trends becoming significant at 1σ or 2σ levels during winter and spring in both hemispheres. Here we consider three distinct seasons where the trends by month for channel 10 (Figure 3) are significantly different from zero at least at 1σ level—December–January–February, April and September–October—and provide the respective latitude-altitude trend patterns in Figure 5. At 1 km vertical resolution, the patterns reveal remarkable altitude variation of the seasonal trends. The layers of (2σ) significant cooling and warming emerge in the tropics, that is, where the broad-resolution channel 10 trends were significant only at 1σ level (Figures 3b and 3c).

During the early austral spring (Figure 5a) a cooling of Antarctic middle stratosphere is accompanied by a warming in the deep tropical lower stratosphere. Given the leveling of Antarctic ozone since 1998 [*Harris et al.*, 2015], such pattern represents a typical signature of the weakening of SH branch of BDC. The same inference can be drawn for NH winter, showing a cooling throughout the polar stratosphere contrasted by a warming in the tropical LS (Figure 5b). An opposite behavior is observed in NH spring; a cooling feature in the tropical LS extending toward midlatitude upper layers is accompanied by a strong warming at northern high latitudes (Figure 5c), i.e., a signature of BDC acceleration. The trend patterns for any other seasons (not shown) do not reveal any coherent structure at the 95% confidence level.

5. Discussion and Summary

An important result of this study is the excellent agreement between AMSU and GPS-RO data records, providing nearly identical trend values and their spatial/seasonal patterns. This is particularly remarkable given that the GPS-RO record incorporates 10 satellite instruments, and the amount of RO observations differs by an order of magnitude before and after 2006. Our results provide confidence in both data sets and confirm that GPS-RO is fully suitable for accurate stratospheric temperature change detection, as already suggested by a number of studies quoted hereinabove.

Intercomparison of lower stratospheric (A)MSU and GPS-RO climatologies by *Steiner et al.* [2007, 2011] and *Ladstädter et al.* [2011] showed significant differences in near-global trend values of up to 0.22 K/decade, and this discrepancy was presumed to stem from the combined MSU-AMSU data record. Here we benefit from the single-satellite Aqua AMSU data set featuring certain advantages [*Funatsu et al.*, 2016] and matching well the GPS-RO time span. After a proper setup of comparable data, the differences in the global trend values from GPS-RO and Aqua AMSU are below 0.05 K/decade.

Various observation-based studies report that despite the leveling of ozone trends [*Harris et al.*, 2015], the stratosphere continued to cool in the 21st century and this change is generally associated with the increase of greenhouse gases [*Stolarski et al.*, 2010; *Seidel et al.*, 2011]. However, the cooling of the middle and upper stratosphere has slowed down after 1997 [*Randel et al.*, 2016], whereas the trends in the lower stratosphere have become insignificantly small [*Seidel et al.*, 2016] most likely due to reversal of the trends in ozone depleting substances [*Polvani et al.*, 2017]. Our analysis of two independent CDRs suggests that the middle stratosphere (AMSU channels 10–12) has cooled in the time period 2002–2016 at an average rate of -0.14 ± 0.12 to -0.36 ± 0.14 K/decade, whereas the statistically significant change in the LS temperature is restricted to certain seasons and latitudes. This inference is consistent with *Randel et al.* [2016] and *Zou and Qian* [2016] reporting respectively -0.23 ± 0.05 and -0.25 ± 0.07 K/decade cooling for SSU-1 (corresponding roughly to AMSU channels 11 and 12) during 1998–2015 and insignificant change for MSU-4 (corresponding to AMSU-9).

While the stratosphere's cooling trend increasing toward its upper layers is a robust feature observed before and after 1998 as well as during shorter periods after 2000 [*McLandress et al.*, 2015; *Funatsu et al.*, 2016], the meridional and seasonal trend patterns appear highly dependent on the time period. In particular, the season-latitude repartition of the trends (Figure 3) characteristic of Arctic cooling (warming) during boreal winter (spring), together with Antarctic cooling during austral spring, is inverse to what was reported for longer time periods.

Analysis of MSU-4 data spanning 1979–2008 by *Fu et al.* [2010] revealed a warming in the Arctic in December–February contrasted by a cooling in spring, which was attributed to strengthening of BDC in winter at both hemispheres and weakening of its NH counterpart in spring. A similar inference was drawn

by *Free* [2011] and *Young et al.* [2012] from MSU-4 data over respectively 1979–2009 and 1979–2005 periods. If the reported trend patterns are indeed representative of the seasonally variable change in BDC strength, then the latter must have reversed its sign in the 21st century as suggested by AMSU and GPS-RO records. The reason for this reversal is unclear, and its robustness is likely limited by the relatively short (compared to SSU/MSU record) 16 year period of GPS-RO observations. Nevertheless, we note that the coherent trend patterns during 2001–2016, presumably reflecting the dynamical change, are statistically significant at 2σ level. Interestingly, *Randel et al.* [2016] showed that the seasonal pattern of trend becomes mostly insignificant after extension of MSU-4 record to 2015, whereas *Osso et al.* [2015] concluded that MSU/SSU observations since 1979 do not reveal any significant trends in BDC.

The complexity of spatial and seasonal structures of stratospheric temperature trend and their dependence on the time period are caused by a combination of different forcings, both natural and anthropogenic. These are carbon dioxide, ozone-depleting substances, ozone, water vapor, solar flux, aerosol load, and sea surface temperature as well as El Niño–Southern Oscillation (ENSO), Quasi-Biennial Oscillation (QBO), and sudden stratospheric warmings. Because these parameters vary in time and some of them are correlated [*Seidel et al.*, 2011], isolating their effects on stratospheric temperatures is highly challenging and prone to large uncertainties, particularly for a relatively short period of time such as the one covered by this study.

A key outcome of this study is the remarkable coherence in trends derived from AMSU and GPS-RO despite the hugely different measurement techniques exploited by those systems. The GPS-RO technique, being fully suitable for benchmark-quality long-term climate monitoring, provides a more detailed view of the lower stratospheric temperature change, thereby allowing a better understanding of the underlying forcing mechanisms using climate models. Future RO missions will continue the existing record, potentially becoming the primary source of information on the lower stratospheric temperature in the 21st century.

Acknowledgments
The AMSU-A CDR was acquired from NOAA's National Climate Data Center (http://www.ncdc.noaa.gov). This study was partly supported by the EU H2020 project ARISE2 (Atmospheric dynamics Research InfraStructure in Europe) and is a contribution to the SPARC Atmospheric Temperature Change Group. H. Gleisner, J. K. Nielsen, S. Syndergaard, and K. B. Lauritsen were supported by the ROM SAF—a decentralized operational RO processing center under EUMETSAT. The reprocessed GPS-RO data, which are part of a coming official CDR V1.0 from the ROM SAF, are available upon request at http://www.romsaf.org. The RO excess phase, amplitude, and orbit data were downloaded from CDAAC/UCAR (http://cdaac-www.cosmic.ucar.edu/cdaac/products.html). We thank Cheng-Zhi Zou at NOAA for providing AMSU weighting functions.

References

Anthes, R. A., et al. (2008), The COSMIC/FORMOSAT-3 mission: Early results, *Bull. Am. Meteorol. Soc.*, *89*, 313–333, doi:10.1175/BAMS-89-3-313.

Beyerle, G., T. Schmidt, G. Michalak, S. Heise, J. Wickert, and C. Reigber (2005), GPS radio occultation with GRACE: Atmospheric profiling utilizing the zero difference technique, *Geophys. Res. Lett.*, *32*, L13806, doi:10.1029/2005GL023109.

Foelsche, U., M. Borsche, A. K. Steiner, A. Gobiet, B. Pirscher, G. Kirchengast, J. Wickert, and T. Schmidt (2008), Observing upper troposphere–lower stratosphere climate with radio occultation data from the CHAMP satellite, *Clim. Dyn.*, *31*, 49–65, doi:10.1007/s00382-007-0337-7.

Foelsche, U., B. Pirscher, M. Borsche, A. K. Steiner, G. Kirchengast, and C. Rocken (2009), Climatologies based on radio occultation data from CHAMP and Formosat-3/COSMIC, in *New Horizons in Occultation Research: Studies in Atmosphere and Climate*, edited by A. K. Steiner et al., pp. 181–194, Springer, Berlin, doi:10.1007/978-3-642-00321-9_15.

Foelsche, U., B. Scherllin-Pirscher, F. Ladstädter, A. K. Steiner, and G. Kirchengast (2011), Refractivity and temperature climate records from multiple radio occultation satellites consistent within 0.05%, *Atmos. Meas. Tech.*, *4*, 2007–2018, doi:10.5194/amt-4-2007-2011.

Free, M. (2011), The seasonal structure of temperature trends in the tropical lower stratosphere, *J. Clim.*, *24*, 859–866.

Fu, Q., S. Solomon, and P. Lin (2010), On the seasonal dependence of tropical lower-stratospheric temperature trends, *Atmos. Chem. Phys.*, *10*, 2643–2653.

Funatsu, B. M., C. Claud, P. Keckhut, A. Hauchecorne, and T. Leblanc (2016), Regional and seasonal stratospheric temperature trends in the last decade (2002–2014) from AMSU observations, *J. Geophys. Res. Atmos.*, *121*, 8172–8185, doi:10.1002/2015JD024305.

Harris, N. R. P., et al. (2015), Past changes in the vertical distribution of ozone – Part 3: Analysis and interpretation of trends, *Atmos. Chem. Phys.*, *15*, 9965–9982, doi:10.5194/acp-15-9965-2015.

Ho, S.-P., et al. (2009), *Estimating the Uncertainty of Using GPS RO Data for Climate Monitoring: Inter-Comparison of CHAMP Refractivity Climate Records 2002–2006 from Different Data*.

Holton, J. R., P. H. Haynes, M. E. McIntyre, A. R. Douglass, R. B. Rood, and L. Pfister (1995), Stratosphere-troposphere exchange, *Rev. Geophys.*, *33*, 403–439, doi:10.1029/95RG02097.

Keckhut, P., B. M. Funatsu, C. Claud, and A. Hauchecorne (2015), Tidal effects on stratospheric temperature series derived from successive advanced microwave sounding units, *Q. J. R. Meteorol. Soc.*, *141*, 477–483, doi:10.1002/qj.2368.

Kursinski, E. R., G. A. Hajj, K. R. Hardy, J. T. Schofield, and R. Linfield (1997), Observing the Earth's atmosphere with radio occultation measurements using the Global Positioning System, *J. Geophys. Res.*, *102*, 23,429–23,465, doi:10.1029/97JD01569.

Ladstädter, F., A. K. Steiner, U. Foelsche, L. Haimberger, C. Tavolato, and G. Kirchengast (2011), An assessment of differences in lower stratospheric temperature records from (a)MSU, radiosondes, and GPS radio occultation, *Atmos. Meas. Tech.*, *4*, 1965–1977, doi:10.5194/amt-4-1965-2011.

Leroy, S. S., J. G. Anderson, and J. A. Dykema (2006), Climate benchmarking using GNSS occultation, in *Atmosphere and Climate: Studies by Occultation Methods*, edited by U. Foelsche, G. Kirchengast, and A. K. Steiner, pp. 287–301, Springer, Berlin.

Luntama, J.-P., G. Kirchengast, M. Borsche, U. Foelsche, A. Steiner, S. Healy, A. von Engeln, E. O'Clerigh, and C. Marquardt (2008), Prospects of the EPS GRAS mission for operational atmospheric applications, *Bull. Am. Meteorol. Soc.*, *89*(12), 1863–1875.

McLandress, C., T. S. Shepherd, A. I. Jonsson, T. von Clarmann, and B. Funke (2015), A method for merging nadir-sounding climate records, with an application to the global-mean stratospheric temperature data sets from SSU and AMSU, *Atmos. Chem. Phys.*, *15*, 9271–9284, doi:10.5194/acp-15-9271-2015.

Osso, A., Y. Sola, K. Rosenlof, B. Hassler, J. Bech, and J. Lorente (2015), How robust are trends in the Brewer–Dobson circulation derived from observed stratospheric temperatures?, *J. Clim.*, *28*, 3024–3040.

Polvani, L. M., L. Wang, V. Aquila, and D. W. Waugh (2017), The impact of ozone-depleting substances on tropical upwelling, as revealed by the absence of lower-stratospheric cooling since the late 1990s, *J. Clim.*, *30*, 2523–2534, doi:10.1175/JCLI-D-16-0532.1.
Ramaswamy, V., et al. (2001), Stratospheric temperature trends: Observations and model simulations, *Rev. Geophys.*, *39*, 71–122.
Randel, W. J., et al. (2009), An update of observed stratospheric temperature trends, *J. Geophys. Res.*, *114*, D02107, doi:10.1029/2008JD010421.
Randel, W. J., A. K. Smith, F. Wu, C.-Z. Zhou, and H. Qian (2016), Stratospheric temperature trends over 1979–2015 derived from combined SSU, MLS, and SABER satellite observations, *J. Clim.*, *29*, 4843–4859, doi:10.1175/JCLI-D-15-0629.1.
Rousseeuw, P. J., and A. M. Leroy (2005), *Robust Regression and Outlier Detection*, vol. 589, John Wiley, Hoboken, N. J.
Scherllin-Pirscher, B., G. Kirchengast, A. K. Steiner, Y.-H. Kuo, and U. Foelsche (2011), Quantifying uncertainty in climatological fields from GPS radio occultation: An empirical-analytical error model, *Atmos. Meas. Tech.*, *4*, 2019–2034, doi:10.5194/amt-4-2019-2011.
Seidel, D. J., N. P. Gillett, J. R. Lanzante, K. P. Shine, and P. W. Thorne (2011), Stratospheric temperature trends: Our evolving understanding, *Wiley Interdiscip. Rev. Clim. Change*, *2*, 592–616, doi:10.1002/wcc.125.
Seidel, D. J., J. Li, C. Mears, I. Moradi, J. Nash, W. J. Randel, R. Saunders, D. W. J. Thompson, and C.-Z. Zou (2016), Stratospheric temperature changes during the satellite era, *J. Geophys. Res. Atmos.*, *121*, 664–681, doi:10.1002/2015JD024039.
Shine, K. P. (1987), The middle atmosphere in the absence of dynamical heat fluxes, *Q. J. R. Meteorol. Soc.*, *113*, 603–633.
Steiner, A. K., G. Kirchengast, and H. P. Ladreiter (1999), Inversion, error analysis, and validation of GPS/MET occultation data, *Ann. Geophys.*, *17*, 122–138, doi:10.1007/s00585-999-0122-5.
Steiner, A. K., G. Kirchengast, M. Borsche, U. Foelsche, and T. Schoengassner (2007), A multi-year comparison of lower stratospheric temperatures from CHAMP radio occultation data with MSU/AMSU records, *J. Geophys. Res.*, *112*, D22110, doi:10.1029/2006JD008283.
Steiner, A. K., G. Kirchengast, B. C. Lackner, B. Pirscher, M. Borsche, and U. Foelsche (2009), Atmospheric temperature change detection with GPS radio occultation 1995 to 2008, *Geophys. Res. Lett.*, *36*, L18702, doi:10.1029/2009GL039777.
Steiner, A. K., B. C. Lackner, F. Ladstädter, B. Scherllin-Pirscher, U. Foelsche, and G. Kirchengast (2011), GPS radio occultation for climate monitoring and change detection, *Radio Sci.*, *46*, RS0D24, doi:10.1029/2010RS004614.
Stolarski, R. S., A. R. Douglass, P. A. Newman, S. Pawson, and M. R. Schoeberl (2010), Relative contribution of greenhouse gases and ozone-depleting substances to temperature trends in the stratosphere: Achemistry–climate model study, *J. Clim.*, *23*, 28–42, doi:10.1175/2009JCLI2955.1.
Thompson, D. W. J., and S. Solomon (2005), Recent stratospheric climate trends as evidenced in radiosonde data: Global structure and tropospheric linkages, *J. Clim.*, *18*, 4785–4795.
Thompson, D. W. J., D. J. Seidel, W. J. Randel, C.-Z. Zou, A. H. Butler, R. Lin, C. Long, C. Mears, and A. Osso (2012), The mystery of recent stratospheric temperature trends, *Nature*, *491*, 692–697, doi:10.1038/nature11579.
Thorne, P. W., J. R. Lanzante, T. C. Peterson, and D. J. Seidel (2010), Shine KP. Tropospheric temperature trends: History of an ongoing controversy, *WIREs: Clim Change*, *2010*(2), 66–88, doi:10.1002/wcc.80.
Wang, W., and C.-Z. Zou (2014), AMSU-A-only atmospheric temperature data records from the lower troposphere to the top of the stratosphere, *J. Atmos. Oceanic Technol.*, *31*(4), 808–825.
Wickert, J., T. Schmidt, G. Beyerle, R. Konig, C. Reigber, and N. Jakowski (2004), The radio occultation experiment aboard CHAMP: Operational data analysis and validation of vertical atmospheric profiles, *J. Meteorol. Soc. Jpn.*, *82*, 381–395.
Young, P. J., K. H. Rosenlof, S. Solomon, S. C. Sherwood, Q. Fu, and J.-F. Lamarque (2012), Changes in stratospheric temperatures and their implications for changes in the Brewer-Dobson circulation, 1979–2005, *J. Clim.*, *25*, 759–1772, doi:10.1175/2011JCLI4048.1.
Yulaeva, E., J. R. Holton, and J. M. Wallace (1994), On the cause of the annual cycle in tropical lower-stratospheric temperatures, *J. Atmos. Sci.*, *51*, 169–174.
Zou, C.-Z., and W. H. Wang (2011), Intersatellite calibration of AMSU-A observations for weather and climate applications, *J. Geophys. Res*, *116*, D23113, doi:10.1029/2011JD016205.
Zou, C.-Z., W. Wang, and NOAA CDR Program (2013), NOAA Fundamental Climate Data Record (FCDR) of AMSU-A Level 1c Brightness Temperature, Version 1.0. [data subset: All data from 2002–2014], NOAA National Climatic Data Center, doi:10.7289/V5X63JT2, [access date: 26/12/2015].
Zou, C.-Z., H. Qian, W. Wang, L. Wang, and C. Long (2014), Recalibration and merging of SSU observations for stratospheric temperature trend studies, *J. Geophys. Res. Atmos.*, *119*, 13,180–13,205, doi:10.1002/2014JD021603.
Zou, C., and H. Qian (2016), Stratospheric temperature climate data record from merged SSU and AMSU-A observations, *J. Atmos. Oceanic Technol.*, *33*, 1967–1984, doi:10.1175/JTECH-D-16-0018.1.